THE JOURNAL OF BIOLOGICAL CHEMISTRY VOL. 283, NO. 52, pp. 36743–36751, December 26, 2008

Native R-loops Persist throughout the Mouse Mitochondrial DNA Genome*[S]

Received for publication, August 11, 2008, and in revised form, November 4, 2008 Published, JBC Papers in Press, November 5, 2008, DOI 10.1074/jbc.M806174200

Timothy A. Brown, Ariana N. Tkachuk, and David A. Clayton[1]

From the Janelia Farm Research Campus, Howard Hughes Medical Institute, Ashburn, Virginia 20147

Mammalian mtDNA has been found here to harbor RNA-DNA hybrids at a variety of locations throughout the genome. The R-loop, previously characterized *in vitro* at the leading strand replication origin (O_H), is isolated as a native RNA-DNA hybrid copurifying with mtDNA. Surprisingly, other mitochondrial transcripts also form stable partial R-loops. These are abundant and affect mtDNA conformation. Current models regarding the mechanism of mammalian mtDNA replication have been expanded by recent data and discordant hypotheses. The presence of stable, nonreplicative, and partially hybridized RNA on the mtDNA template is significant for the reevaluation of replication models based on two-dimensional agarose gel analyses. In addition, the close association of a subpopulation of mtRNA with the DNA template has further implications regarding the structure, maintenance, and expression of the mitochondrial genome. These results demonstrate that variously processed and targeted mtRNAs within mammalian mitochondria likely have multiple functions in addition to their conventional roles.

The normal fate of an RNA transcript is to exit the transcription complex and proceed to its functional site in the cell. An exception is the retention of the RNA paired to its DNA template complement as an RNA-DNA hybrid. These RNA-DNA hybrids, or R-loops, are typically found at origins of DNA replication. An early example of this phenomenon is the plasmid ColE1 replication origin in *Escherichia coli*, where R-loops are formed during transcription and then processed into shorter primers that sponsor DNA replication (1). A similar RNA-DNA hybrid is also utilized at the mammalian mtDNA replication origin, O_H.[2] Here, transcription from the light-strand promoter creates an RNA-DNA hybrid, which is a substrate for the endoribonuclease complex RNase MRP. The RNA processing sites for this nuclease coincide with RNA to DNA transitions, implicating a role in generating replication primers from the O_H R-loop (2, 3). The R-loops at mtDNA origins from yeast, mouse, and human have been reconstituted and characterized *in vitro* (2, 4, 5).

Replication of mammalian mtDNA proceeds by a displacement mode of replication utilizing origins that are strand-specific and asymmetrically positioned (Fig. 1). After initiation at O_H, unidirectional synthesis proceeds along the template while displacing the opposite strand up to a distance of about two-thirds around the 16-kb circular genome. Here, the nascent strand reaches the opposite strand-specific origin, O_L, where synthesis of the second strand initiates. Elongation of the second strand then continues along the previously displaced single-stranded template in the opposite direction. Both strands are extended in an asymmetric manner until two daughter molecules are formed (6, 7).

Recently, we and others have proposed alternative modes of mtDNA replication with initiation sites in addition to the site-specific origins described initially (8–11). Specifically, we have proposed that light-strand replication initiation can occur at various locations other than O_L, as alternative light-strand origins ($^{alt}O_L$) (10, 11). This $^{alt}O_L$ modification of the standard model only requires, on occasion, a reduction in the asymmetry and a mechanism to initiate light-strand replication at locations other than O_L. We believe that this model is most consistent with the current total available data.

We therefore initiated a search for stable primer RNAs at various locations within the mouse mtDNA genome. We found that primer R-loops at O_H are indeed stable enough to co-purify with mtDNA. These RNA primers at O_H confirm the position of the major replication initiation site, as well as indicating other novel, but less prominent, initiation sites further downstream. We also found RNAs associated with mtDNA at positions that could potentially function as $^{alt}O_L$ primers. Sequence analysis revealed that some of the R-loops located at the COII gene had a free 3′-OH, which would make them viable substrates for extension by mtDNA polymerase. Yet, unlike the R-loop at O_H, RNAs from the gene transcript R-loops were not sensitive to DNase, indicating that they are not frequently used as replication primers. This is in agreement with imaging data of replicative intermediates (10, 12).

Surprisingly, we also found that other mtRNAs remained bound to mtDNA that were unlikely to be involved in DNA replication priming. These RNAs were large, pervasive, variously processed, occurred on both strands, and appeared to associate with the mtDNA in a manner that restricted the conformation of the supercoiled DNA. The finding that R-loops

* The costs of publication of this article were defrayed in part by the payment of page charges. This article must therefore be hereby marked "*advertisement*" in accordance with 18 U.S.C. Section 1734 solely to indicate this fact.

[S] The on-line version of this article (available at http://www.jbc.org) contains supplemental Figs. S1 and S2.

⌘ *Author's Choice*—Final version full access.

[1] To whom correspondence should be addressed: 19700 Helix Dr., Ashburn, VA 20147-2408. Fax: 571-209-4059; E-mail: claytond@janelia.hhmi.org.

[2] The abbreviations used are: O_H, heavy-strand origin of replication; O_L, light-strand origin of replication; $^{alt}O_L$, alternative light-strand origin; Cyt *b*, cytochrome *b*; COII, cytochrome oxidase subunit II; ND1 and ND6, NADH dehydrogenase complex subunits 1 and 6; DIG, digoxigenin; CSB, conserved sequence block; AFM, atomic force microscopy; RITOLS, RNA incorporation throughout the light strand; DEPC, diethylpyrocarbonate; RT, reverse transcription; RACE, rapid amplification of cDNA ends; ANOVA, analysis of variance; nt, nucleotide(s).

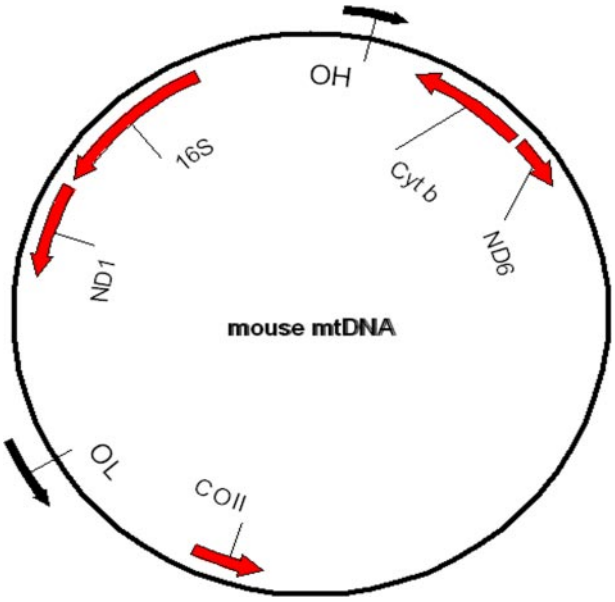

FIGURE 1. **Map of mouse mtDNA.** The circular genome is ~16.3 kb. The two strand-specific origins (O_H and O_L) are designated by *black arrows* around the outside of the map. Displacement replication exposes a single H-strand between O_H and O_L containing the Cyt *b*, ND6, and COII genes. The control region encompassing O_H is shown in greater detail in Fig. 2. Genes with transcripts analyzed in this work include 16S rRNA, ND1, COII, ND6, and Cyt *b* and appear as *bold red arrows*. Other mitochondrial genes were excluded for clarity.

were stably bound to mtDNA throughout the genome was unexpected yet was consistent with earlier reports indicating that RNA is closely associated with mtDNA *in vivo*. These R-loops may be present in some of the mtDNA forms that have been characterized as replication intermediates in two-dimensional agarose gels (9). In contrast to that analysis, however, our results indicate that the R-loops are discrete, heterogeneous, mtDNA gene transcripts and not principally replication intermediates. Pervasive, heterogeneous, and stable mtDNA transcript R-loops provide a basis for the RNA-influenced two-dimensional agarose gel patterns that is independent of active mtDNA replication.

Mitochondrial R-loops have features that likely indicate multiple roles in the maintenance and expression of the genome. These include priming of replication at the leading strand origin of replication (O_H) and, potentially, at alternative light-strand replication initiation sites. R-looped RNAs also demonstrate an ability to alter the conformation of mtDNA, implying a larger structural role within the mitochondrial nucleoid. Outside of the mitochondria, R-loops have been shown to have both positive and negative consequences. In mammalian immune cells, R-loops mediate DNA recombination en route to immunoglobulin class switching (13). In yeast, excessive R-loop formation causes harmful recombination (14). In *E. coli*, R-loops sponsor replication initiation (15) and are also thought to limit bacterial growth and inhibit transcription outside of replication origins (16). Alternatively, bacterial R-loops are hypothesized to support the repair of arrested replication forks (17). The full roles or consequences of such noncoding functions of RNA within mammalian mitochondria deserve renewed consideration.

EXPERIMENTAL PROCEDURES

Isolation of mtDNA-mtRNA Complexes—Isolation of mtDNA-mtRNA from the mouse cell line LA9 was accomplished using the differential centrifugation and ethidium bromide-cesium chloride (EtBr-CsCl) gradient method described previously (18). Mouse liver mtDNA-mtRNA was also isolated using sucrose and EtBr-CsCl gradients as described previously (10). Purified nucleic acid complexes were kept at 4 °C in CsCl prior to analysis. An image of such a gradient is shown in supplemental Fig. S1. At the top of the gradient is the protein film. The wide fluorescent band lower in the tube is contaminating linear DNA, which is almost entirely nuclear. The amount of contaminating nuclear DNA did not change substantially whether the mitochondria were isolated using differential centrifugation or sucrose gradients. Below this is the closed circular mtDNA, which represents at most 1/50th of the total DNA in the tube. RNA sediments as a pellet at the bottom of these CsCl gradients. This pellet was reconstituted in DEPC-treated water and used as a source of total mtRNA. RNA and DNA were quantified using a Nanodrop ND-1000 and used directly for both RT-PCR and Northern blot assays. Poly(A)+ purified RNA was isolated from 10^7 LA9 cells preserved in RNAlater reagent using first the RNAqueous kit and then the MicroPoly(A)Purist kit (Ambion). This Poly(A)+ purified RNA was used as a control for both RT-PCR and Northern blot analysis. For the mtDNA-mtRNA co-fractionation analysis, a 19-gauge safety-winged infusion set needle (Terumo) was inserted 1.5 cm below the lower (mtDNA) band in the EtBr-CsCl gradient tube. Five drop fractions were collected, and 100-μl samples were dialyzed in DEPC-treated phosphate-buffered saline at 4 °C for 20 h. Slide-A-Lyzer MINI dialysis units (Pierce, molecular weight cut-off 7000) were first pretreated with DEPC-phosphate-buffered saline. Postdialysis volumes were noted to correct for dilution of the samples. Mitochondrial DNA concentration was determined using a validated quantitative PCR method described previously using the Roche LightCycler apparatus (19). RNA was quantified with the Quant-iT^{TM} RiboGreen RNA reagent kit (Molecular Probes) using the supplier's instructions. Samples were pretreated with RNase-free DNase I (Ambion) as instructed to eliminate any signal due to DNA dye binding. Replicates and dilutions were done in a 96-well plate format and read using a Tecan Safire^{2TM} plate reader.

Digoxigenin (DIG) RNA Probes for Northern Blots—DIG-labeled, single-stranded RNA probes were synthesized by direct *in vitro* transcription of DNA templates obtained by PCR using gene-specific primers containing consensus sequences for T7 and T3 RNA polymerase promoters and incorporating DIG-11-UTP (Roche Applied Science). The plasmid p501-1, containing the entire mouse mitochondrial genome sequence, was used as the template and subsequent PCR products were isolated by agarose electrophoresis and gel extraction using a modified freeze-squeeze method (20). T3 or T7 promoter-driven RNA probes were transcribed per the manufacturer's instructions (Roche Applied Science) with two modifications: 40 units of Protector RNase Inhibitor was added per reaction, and the incubation was done for 1 h at 42 °C.

Primers used for RNA probe template generation were: T7 ND1, 5′-ccaagcttctaatacgactcactatagggagacggaagcgtggataagatg-3′; T3 ND1, 5′-cagagatgcaattaaccctcactaaagggagaggcccattcgcgttattc-3′; T7 ND6, 5′-ccaagcttctaatacgactcactatagggagagctactgaggaatatccaga-3′; T3 ND6, 5′-cagagatgcaattaaccctcactaaagggagactccaacatcatcaacctca-3′; T7 CytB, 5′-ccaagcttctaatacgactcactatagggagacgaagaatcgggtcaaggt-3′; T3 CytB, 5′-cagagatgcaattaaccctcactaaagggagatcgcagtcatagccacagc-3′; T7 COII, 5′-ccaagcttctaatacgactcactatagggagaatttagtcggcctgggatg-3′; T3 COII, 5′-cagagatgcaattaaccctcactaaagggagaccgagtcgttctgccaata-3′; T7 16S, 5′-ccaagcttctaatacgactcactatagggagagaccctcgtttagccgttc-3′; T3 16S, 5′-cagagatgcaattaaccctcactaaagggagactgcctgcccagtgactaa-3′; T7-4, 5′-ccaagcttctaatacgactcactatagggagagatcaggacatagggtttg-3′; T3-4, 5′-cagagatgcaattaaccctcactaaagggagacataaatgctactcaatac-3′; T3-1 (T3dloop1), 5′-cagagatgcaattaaccctcactaaagggagaaatcagcccatgaccaaca-3′; 3′-DloopRNA1, 5′-ggactaatgattcttcaccgtagg-3′.

Northern Analysis—Purified mtDNA-mtRNA was first desalted to ~200–400 mM CsCl by ultrafiltration and dilution with DEPC-treated water using Amicon Ultra-4 (molecular weight cut-off 100,000) centrifugal filters. Nucleic acids were then ethanol-precipitated and dissolved in 20–30 μl of citrate buffer. 500 ng of LA9 mtDNA-mtRNA were treated with 1.4 units of RNase-free DNase I (Ambion) or RNase H (Stratagene), denatured with glyoxal/DMSO, and separated on a 1% agarose gel using the NorthernMax-Gly kit (Ambion). Downward capillary transfer was completed per the manufacturer's instructions, substituting positively charged nylon membranes (Roche Applied Science), and RNA was UV-cross-linked to the membrane (1200 × 100 μJ/cm^2, Spectronics). Northern blots were prehybridized for 30 min and then hybridized overnight at 68 °C with DIG-labeled antisense RNA probes using the DIG Northern Kit (Roche Applied Science). CDP-Star was used for immunological chemiluminescent detection of the DIG-labeled RNA. Blots were exposed to x-ray film for visualizing the RNA bands. 100 ng of poly(A)+ purified mRNA was used per lane as a probe control.

mtRNA Guanylation or Circularization—Ethanol-precipitated mtDNA-mtRNA hybrids and total RNA pellet samples (1–4 μg) were treated with TURBO DNase I using the DNA-free rigorous protocol (Ambion) and circularized using T4 RNA ligase or polyguanylated using the poly(A) tailing kit with *E. coli* poly(A) polymerase (E-PAP; Ambion) per the manufacturer's instructions, with the following modifications for the guanylation. Samples were incubated for 1 h at 37 °C with 1 mM ribo-GTP in a 50-μl reaction mixture, which was then purified using the MEGAclear kit (Ambion) before RT-PCR. RNA guanylation RT-PCR analysis was similar to that of Kusov *et al.* (21).

Rapid Amplification of cDNA Ends (RACE)—RT-PCR was done using the FirstChoice RLM-RACE kit (Ambion) to amplify both the 5′- and 3′-ends of the polyguanylated RNA samples with the following modifications. Calf intestine alkaline phosphatase and tobacco acid pyrophosphatase treatments were omitted from 5′-RACE prior to ligation of the 5′-RACE adaptor (Ambion). The gene-specific primer 4FS (5′-cgtagagaggggagagcaattatg-3′) was used for 5′-RT of the COII gene. The universal primer 3′-RACE oligo(dC) linker (5′-gctgtcaacgatacgctacgtaacggcatgacagtgccccccccccc-3′) was used for 3′-RT of the COII and Cyt *b* genes. RT-PCR across the 3′-to-5′ junction was done on the circularized RNA samples using HIV-1 reverse transcriptase (Ambion). This assay is similar to that used by Tomecki *et al.* (22). First strand cDNA synthesis was accomplished using 3′-RACE COII nested (5′-ctgccaatagaacttccaatcc-3′) as the primer. Samples and primer were first denatured at 70 °C for 3 min and reverse transcribed at 50 °C for 1 h. The RT reaction was stopped by heat inactivation at 92 °C for 10 min. All cDNA products were PCR-amplified using PlatinumTaq DNA polymerase (Invitrogen). Amplification of the 5′-end of the COII gene was done using 5′-RACE Outer (Ambion) as the forward primer and 4FS or 4N (5′-taggggatgtggcgtcttgt-3′) as the reverse. 3′-End amplification was done using Generacer 3′ (Ambion) as the reverse primer and 3′-RACE COII (5′-aagttgataaccgagtcgttctg-3′), 3′-RACE COII nested (5′-ctgccaatagaacttccaatcc-3′). or 3′-RACE COII nested 2 (5′-atcaagcaacagtaacatcaaacc-3′) and 3′-RACE CytB (5′-gccctaataccttttccttcatacc-3′) or 3′-RACE CytB nested (5′-ctaatattccgcccaatcacac-3′) as the gene-specific forward primers for the COII and Cyt *b* genes, respectively. The primers used for amplifying cDNA across the circularized RNA junctions were 3′-RACE COII nested 2 (forward) and 4FS or 4N (reverse) for the COII gene. PCR products were cloned using the pGEM-T Easy vector (Promega) and sequenced with M13for and M13rev primers.

Atomic Force Microscopy—Immobilization of the DNA-protein complexes onto a mica surface was done as described previously (23). Briefly, CsCl-purified mtDNA-mtRNA was desalted, and buffer was exchanged into 4 mM HEPES, 10 mM NaCl, 2 mM $MgCl_2$ as the mica binding buffer using the Amicon Ultra-4 filters described above. DNase-free RNase A purchased from Ambion was used at a final concentration of 0.04 ng/μl for 10 min at 37 °C. A 20-μl volume of mtDNA was applied to freshly exposed mica and allowed to attach for 2 min. The mica surface was washed gently with nuclease-free water and dried under a stream of nitrogen. Microscopy was performed with a Multimode AFM with a Nanoscope IVa controller (Veeco) in tapping mode using tips from Nanosensors (PointProbes, type NCH-20). R-loops were detected using *E. coli* single-stranded DNA-binding protein similar to the detection of D-loops described previously (10). Plasmid p501-1 DNA containing the entire mouse mtDNA genome was purified as described above. Control R-loops using p501-1 were created by first generating a 428-nt single-stranded COII RNA in sense orientation. RNA was created from PCR templates generated from T3 and T7 promoter-containing oligos T3COII2 (5′-cagagatgcaattaaccctcactaaagggagaatggcctacccattccaact-3′) and T7COII2 (5′-ccaagcttctaatacgactcactatagggagacaatgggcataaagctatgg-3′), as outlined above for the synthesis of RNA probes, without use of DIG bases. This RNA was annealed to supercoiled p501-1 plasmid DNA in a 4:1 RNA to DNA molar ratio by heating at 70 °C for 4–6 h in 62% formamide, 25 mM HEPES, pH 7.5, 400 mM NaCl, 1.25 mM EDTA followed by gradual cooling overnight at an initial rate of 8 °C/h and holding to ambient temperature. Buffer exchange and atomic force microscopy (AFM) imaging was done as described above. RNase H treatment was for 30 min at 37 °C with 1 unit in a 20-μl reaction volume. *E. coli* single-

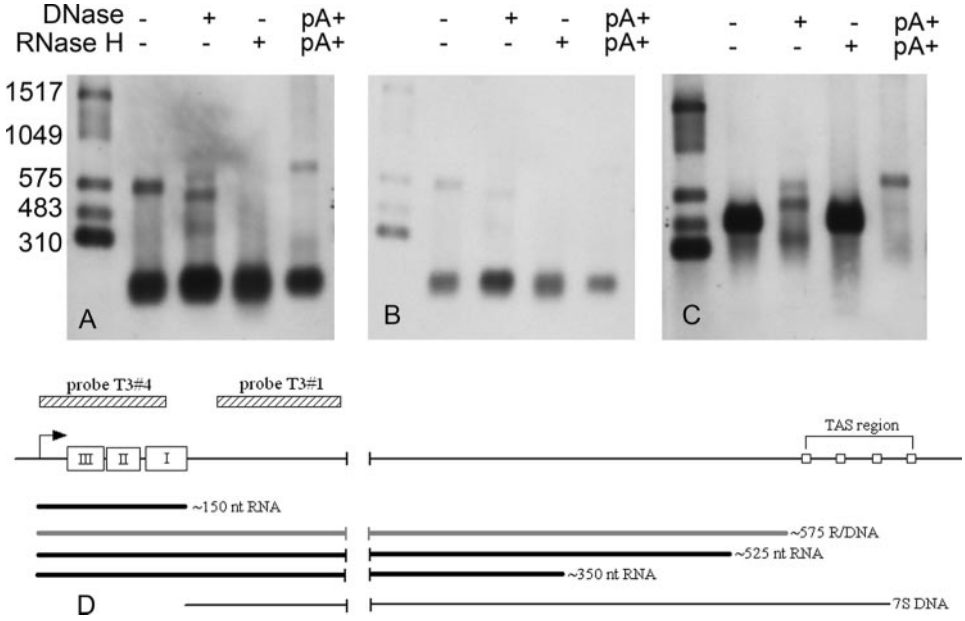

FIGURE 2. **Northern analysis and DNase and RNase sensitivity of mtDNA-bound nascent H-strand RNA and DNA at O_H.** EtBr-CsCl-purified closed circular mtDNA was analyzed by Northern analysis to detect stable R-loops. RNA size markers are in *lane 1*. Poly(A)+-purified RNA is in the *lane* denoted by *pA+*. DNase I and RNase H sample treatments are indicated *above* the *panels*. *A*, probing for CSB-proximal RNA with T3#4 riboprobe (shown in *D*). *B*, less exposed film of view shown in *A*, revealing the increased intensity of ~150-nt species in *lane 3* after DNase treatment. *C*, probing for CSB-distal RNA with T3#1 riboprobe as shown in *D*. *D*, reference diagram showing the major noncoding region of mtDNA. This region is identified in Fig. 1 as the area encompassing O_H. The transcription start site is shown with a *bent arrow* followed by several relevant DNA sequence features, including CSBs III, II, and I. The termination-associated sequences (*TAS*) region is shown at the promoter distal end of the DNA. T3#4 and T#31 riboprobe positions are shown above. Below the DNA map are nucleic acids identified in the Northern blots shown in *A–C*. RNA is shown by *thick black lines*, and RNA primers in transition with DNA are shown in *gray*. DNA alone is in shown by *thin black lines*. The *lines* are to scale, with size interruptions shown by *breaks*.

stranded DNA-binding protein (USB Corp.) was bound to DNA at a final concentration of 1 ng/μl. *In vitro*-generated R-loops were formed on 39% of the molecules screened by random searching under AFM.

RESULTS

Dye-binding-CsCl Gradient Purification of mtDNA and mtRNA—Our goal was to isolate RNA species which were stably associated with mtDNA. Contaminating RNAs could potentially confound the analyses. EtBr-CsCl isopycnic gradient centrifugation remains the standard for obtaining the highest purity of closed circular mtDNA. The technique has been stated as yielding lower quality mtDNA preparations (9) despite evidence to the contrary (10). An image of such a gradient is shown in supplemental Fig. S1. It is noteworthy that mitochondria isolated either by differential or sucrose gradient centrifugation do not yield highly purified mtDNA as obtained by subsequent phenol extraction (24). In fact, the amount of contaminating nuclear DNA co-isolated in such preparations is at least 50 times that of mtDNA (see supplemental Fig. S1). Historically, a nuclease treatment of mitochondria has been employed to lessen the amount of contaminating nuclear DNA (25, 26). Total RNA centrifuging to the bottom of the EtBr-CsCl gradients represents ~100 times that of mtDNA by mass. More importantly, supplemental Fig. S1 shows that a fraction of the total RNA also co-isolates with mtDNA in the EtBr-CsCl gradients. The amount of RNA at the same position as mtDNA in this peak is ~25% of the mtDNA by mass.

Processed Replication Primers at the Heavy-strand Origin Copurify with mtDNA—R-loops on mtDNA were initially characterized using Northern analysis. We probed first for the replication primer RNA at O_H. Our results indicate that primer RNAs at O_H remained stably associated with the DNA template. A schematic of the mtDNA control region containing O_H is shown in Fig. 2*D*. Furthermore, our analysis reveals the major and minor primer RNA to DNA synthesis transition sites in this region. Although the RNA to DNA transition sites were previously shown to be somewhat heterogeneous, in mouse mitochondria the major transition site lies at the promoter distal side of the conserved sequence block CSBI (27, 28), as diagrammed in Fig. 2*D*. The results in Fig. 2*A* show primer RNA at this location detected with probe T3#4. The abundant ~150-nt RNA has a size and sequence consistent with it having a 5′-end at the transcription initiation site and a 3′-end at CSBI, as represented in Fig. 2*D*. The RNA mapping was supported further by additional probing on the distal side of CSBI, as shown in Fig. 2*C*, where the ~150-nt RNA is limited to the CSB region. This ~150-nt RNA was not extensively sensitive to RNase H, indicating that either the processed RNA is hybridized to the DNA over a short terminal sequence or the structure of the hybrid somehow confers resistance to this enzyme. Therefore, an RNA corresponding to the major RNA to DNA transition site at O_H copurifies as a stable R-loop with mtDNA. This RNA also exists in polyadenylated form, as it is abundantly present in the poly(A)+ control lane, perhaps indicating that it is targeted for turnover (29).

In addition to the major ~150-nt RNA, Fig. 2*A* also reveals a larger species of ~575 nt. In contrast, this larger species is sensitive to both RNase H and DNase I, indicating that its length contains both ribo- and deoxyribonucleotides. Therefore, this represents replication intermediates in which the RNA has primed synthesis of DNA and the two remain covalently linked at transition sites. The differential sensitivity to these nucleases indicates that the promoter-proximal CSB portion of this ~575-nt species is composed of RNA. DNase treatment of this species leaves a heterogeneous population of RNA with two distinct bands at ~525 and ~350 nt. Lighter exposure of this Northern blot shows that in fact the most abundant RNA liberated from the DNase-treated ~575-nt species is also ~150 nt (Fig. 2*B*). This is consistent with the existence of the major RNA

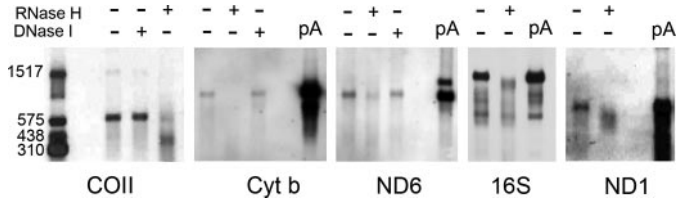

FIGURE 3. **Northern analysis and RNase H and DNase I sensitivity of R-loops within mtDNA coding regions.** Mitochondrial RNA remains bound to CsCl-purified mtDNA. Samples were prepared as described in the legend for Fig. 2 and treated with nucleases as indicated by (+) and (−). *pA* is poly(A)+-purified RNA. Gene-specific riboprobes were generated from PCR products as described under "Experimental Procedures."

to DNA transition site adjacent to CSBI and two discrete but less abundant transitions further downstream. The ~575-nt species therefore represents a heterogeneous length of covalently linked RNA and DNA with transition sites at various and discrete locations along its length. Other minor RNA to DNA transitions sites have been mapped previously at assorted locations in mouse mtDNA, which accounts for much of the heterogeneity indicated by the less discrete, smeared signal (27). However, the more discrete transition sites defined by the DNase-resistant ~525-nt and ~350-nt RNAs lie further away from the CSB region and would have escaped most of the earlier fine mapping efforts. These may represent novel primer-initiated replication start sites.

To differentiate between primer RNA and DNA extensions, we used probe T3#1, as shown in Fig. 2*C*. The major species detected with this probe at ~550 nt is not RNA but rather DNA, as demonstrated by its sensitivity to DNase. This is again consistent with prior data showing that the major RNA to DNA transition occurs at CSBI and that the subsequent DNA strand most often terminates after 540–570 nt, creating the common mitochondrial D-loop structure. This DNA strand is known as 7S DNA (Fig. 2*D*). DNase I treatment also reveals the ~525- and ~350-nt DNase-resistant RNA species seen previously in Fig. 2*A*, confirming that those RNAs are in fact extending beyond the CSB region and that the DNA portion of these strands is located toward the 3′-end.

COII and Cyt b RNAs Also Copurify with mtDNA—We extended our search for primer RNA to a region of the mtDNA thought to contain alternative light-strand origin primers, focusing on the COII and Cyt *b* gene regions. RNAs from both of these regions were found to copurify with mtDNA. Fig. 3 shows that the COII transcript associated with mtDNA is similar in length to the full transcript. Treatment of the sample with DNase I indicates that this RNA has not been extended by DNA polymerase and therefore is not a significant source of replication intermediates. The RNA is only partially sensitive to RNase H, indicating that it is incompletely hybridized to the DNA template in partial R-loop form. Fig. 3 shows similar results are obtained for the major RNA hybridizing to the Cyt *b* probe. Again, this RNA is insensitive to DNase treatment. However, it is more fully sensitive to RNase H, indicating additional extensive hybridization or exposure.

R-looped RNAs Are a Mix of Full-length, Short, and Long Transcripts with Variable 5′- and 3′-Ends—Both RACE and circularized RT-PCR analyses were used to determine whether the partially R-looped COII and Cyt *b* RNAs have distinctive ends. The data are shown in Table 1. The control population of COII poly(A)+ RNA is most consistently full-length at both ends, with poly(A) tails ranging in length from 8 to 56 nucleo-

TABLE 1

Sequence analysis of RNA ends by RACE and RT-PCR

Nucleotide positions are according to the mouse reference sequence NC_005089 and denote positions relative to the reading frame. The 5′- and 3′-ends of COII open reading frame occur at nt 7013 and 7696, respectively. The 5′- and 3′-ends of Cyt *b* open reading frame occur at nt 14,145 and 15,288, respectively. The number of nucleotides relative to these references is shown in parentheses. Bold numerals indicate end positions predicted to have non-aberrant translation. The numbers of replicate clones are italicized and bracketed.

Nucleotide position of 5′-ends	Nucleotide position of 3′-ends	3′ Modification
COII R-loop		
7012 (+1) [*13*]	**7699 (+3)**	A^{5}, A^{17}, A^{20}, A^{23}, A^{44}, A^{44}, A^{45}, A^{46} [*2*], A^{47}, A^{48}, A^{51} [*2*], A^{56}, A^{57}, A^{59}
7013 [*7*]	**7699 (+3)**	UA^{50}
6988 (+25)	**7698 (+2)**	$\mathbf{A^{51}}$
6939 (+74)	**7698 (+2)**	None
	7670 (−26)	None [*4*]
	7656 (−40)	None [*3*]
	7635 (−61)	None
	7630 (−66)	None
	7626 (−70)	None
	7579 (−117)	U^{30}
	7577 (−119)	None [*4*]
COII poly(A)+		
7012 (+2) [*15*]	**7699 (+3)**	A^{8}, A^{9}, A^{10}, A^{12}, A^{13}, A^{14}, A^{16}, A^{22}, A^{24}, A^{37} [*2*], A^{39}, A^{41}, A^{43}, A^{47}, A^{48}, A^{49}, A^{53}, A^{55}, A^{56}
7013 (+1) [*3*]	**7697 (+1)**	A^{17}
	7699 (+3)	A^{14} U A^{25}
	7699 (+3)	A^{6} C A^{47}
COII total RNA		
7012 (+1) [*21*]	**7699 (+3)**	A^{28}, A^{60}, A^{57}, A^{51}, A^{48} [*2*], A^{6} [*2*], A^{45}, A^{44} [*2*], A^{43}, A^{45}, A^{42} [*2*], A^{39}, A^{37}, A^{32}, A^{30}
7013 [*7*]	**7699 (+3)**	None [*2*]
7016 (−3)	**7699 (+3)**	$A^{39}GA^{3}$
7185 (−172)	7722 (+26)	None
7192 (−179)	7710 (+14)	None
7194 (−181)	7631 (−65)	None
	7629 (−67)	None
	7663 (−33)	None
	7633 (−63)	None
	7588 (−108)	None
Cyt *b* R-loop		
14,140 (+5) [*16*]	**15,288**	A^{21}, A^{56}
14,113 (+32)	15,354 (+66)	None [*2*]
14,107 (+38)	15,354 (+66)	U^{22}, U^{8}, U^{7}, U^{2}
14,081 (+64)	15,355 (+67)	$U^{29}CU$
14,026 (+119)	15,355 (+67)	U, U^{3}, U^{5} [*2*], U^{15}
14,022 (+123) [*2*]	15,422 (+134)	None
13,931 (+214)	15,517 (+229)	None [*2*]
13,816 (+329)	15,284 (−4)	None
14,165 (−20) [*2*]	15,265 (−23)	$A^{8}GA^{2}$
14,200 (−55)	15,239 (−49)	U [*2*]
14,216 (−71)	15,213 (−75)	None
14,217 (−72)	15,208 (−80)	None
14,220 (−75)	15,175 (−113)	U^{10} [*2*], U^{17}
14,225 (−80)	15,175 (−113)	None
	15,174 (−114)	$U^{2}AU^{3}$ [*2*]
	15,174 (−114)	U^{6}
	15,174 (−114)	None
	15,172 (−116)	U [*3*]
	15,170 (−118)	None
Cyt *b* total RNA		
14,140 (+5) [*24*]	**15,288**	A^{63}
14,023 (+122) [*2*]	15,280 (+8)	U^{8}
14,003 (+142)	15,355 (+67)	U, U^{2}, U^{4} [3], U^{5} [3], U^{32}
14,146 (−1) [*2*]	15,355 (+67)	$U^{15}GT^{2}$
14,192 (−47)	15,355 (+67)	None
	15,354 (+66)	$GU^{13}GU^{2}$
	15,354 (+66)	None [*5*]
	15,354 (+66)	U, U^{2}, U^{3} [2] U^{4} [3], U^{5}, U^{5}, U^{6}, U^{8}, U^{8}

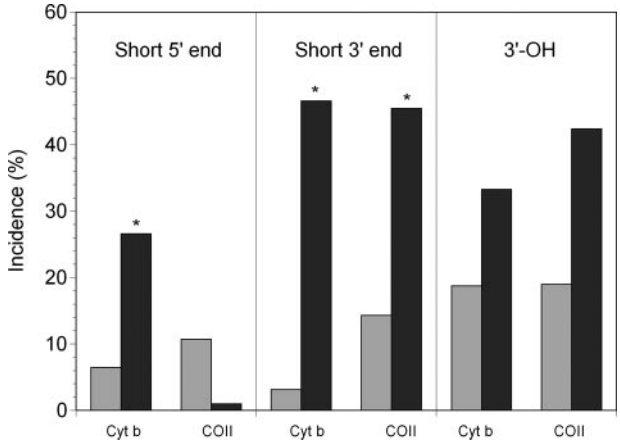

FIGURE 4. **R-loop RNA ends are unlike total RNA ends.** The incidences of short 5′-ends, 3′-ends, and unmodified 3′-ends (3′-OH) are displayed. Incidences within total RNA are shown as *gray bars*, and those within the R-loop population are shown as *black bars*. *Asterisks* indicate a significant difference at $p < 0.05$ using ANOVA. Data are taken from Table 1.

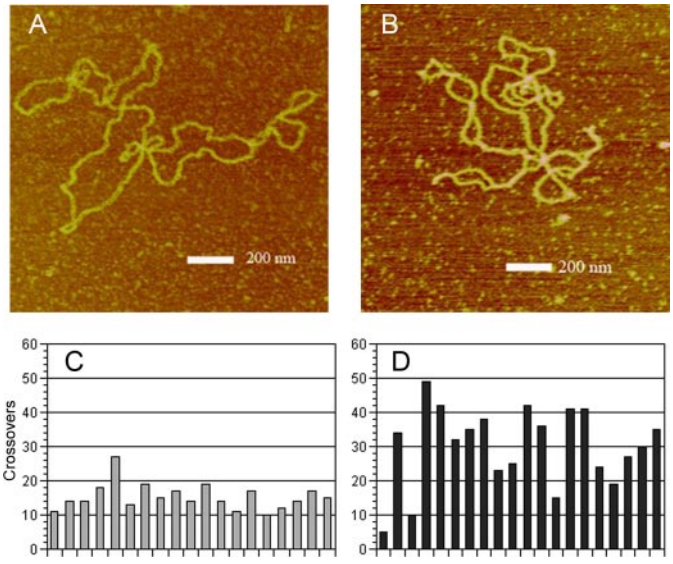

FIGURE 5. **Bound RNA affects mtDNA conformation.** *A* and *B*, AFM imaging of mtDNA before (*A*) and after (*B*) treatment with RNase A. Highly twisted plectoneme structures are seen in several regions of *B* only after removal of the bound RNA. DNA crossovers per molecule are shown in distributed form and as a relative measure of apparent writhe in *C* and *D*. The untreated crossover distribution is shown in *C* with *gray bars*, and the RNase-treated distribution is shown in *D* with *black bars*. Each *bar* represents data for an individual molecule. The median crossover numbers are 14 and 33 for *C* and *D*, respectively. ANOVA single factor analysis indicates a significant difference at $p = 3.1 \times 10^{-5}$.

tides. The mean poly(A) tail is about 31 nucleotides. COII clones that were full-length with respect to the reading frame were also most common in both the total RNA control sample and the DNA-bound R-loop sample. Neither of these samples displayed a high level of heterogeneity at the 5′-end. However, the R-loop sample differed from the total RNA sample by having a higher frequency of COII RNAs that were abbreviated at the 3′-end, as shown in Fig. 4. The Cyt *b* R-loop sample also had a significantly higher frequency of short 3′-ends. Unlike the COII RNAs, the Cyt *b* R-loops also had 5′-ends that were more likely to be either elongated or shorter than the reading frame. Although 3′-end modification is most common, both the total RNA and R-loop samples for both genes displayed numerous clones with unmodified 3′-ends (Fig. 4). Although these were more frequent in the R-loop sample, this difference is not significant. Nevertheless, the R-loop ends display a distinctive distribution that is unlike that of either the total RNA population or the poly(A)+ RNA population.

Sequencing of RACE and Circularized RT-PCR Clones Reveals Unusual Processing of Cyt b Transcripts—The Cyt *b* gene mRNA requires polyadenylation at the appropriately processed site in order to complete a termination codon at the end of the reading frame. However, RNA processing at this site was surprisingly rare, although when it did occur, polyadenylation was found as well. RNA processing at sites other than the end of the Cyt *b*-encoded reading frame was more typical, and uridylation was the common posttranscriptional 3′-end modification. The most common alternate 3′-coded terminus for the Cyt *b* transcript also included the downstream tRNA *Thr* gene sequence. These clones were present in both the total RNA and R-loop samples. It appears that the 5′-end processing of the tRNA, presumably by RNase P, is inefficient at this site. The consequences of this are unclear, but translation of this contiguous transcript would encode a Cyt *b* polypeptide with an additional 11 amino acids at the C terminus prior to translational termination. The significance of the 3′-uridylation is also not obvious. A single polyuridylated clone was also found in the COII R-loop population (Table 1).

Other mtRNAs Also Associate with Purified mtDNA—Because COII and Cyt *b* RNAs were found as R-loops on the mtDNA, we sought to extend our analysis to those regions outside the expected $^{alt}O_L$ region. We found that R-loop formation also occurred at locations that were inconsistent with obvious roles in replication. Fig. 3 shows that the ND6, 16S rRNA, and ND1 RNAs are also associated with mtDNA as partially hybridized R-loops. R-loop formation appears to be a common feature of mitochondrial transcription. Quantification of the RNA and DNA components of EtBr-CsCl purified complex revealed that the two components cofractionate and that the RNA represents ~25% by mass of the complex (supplemental Fig. S1). Assuming that the RNA is largely single-stranded, we might thereby estimate that as much 50% of the mtDNA length is in some form of limited R-loop.

RNA Maintains mtDNA in a More Open Conformation—We visualized mtDNA-RNA complexes using AFM. Fig. 5*A* reveals that the partially R-looped RNA remains associated with mtDNA as a triple-stranded structure and is not readily visible as a third, highly folded strand that is partially dissociated from the DNA. Because prior RNase H sensitivity results (Figs. 2 and 3) indicated that most RNAs are only partially hybridized, this result was unexpected. Nevertheless, extensive searches for loosely associated, folded RNA on the mtDNA contour were unrevealing. We were also unable to detect extensive stretches of RNA-DNA hybrid regions using AFM, which is consistent with the RNase H-sensitive Northern data. Supplemental Fig. S2 shows that AFM can detect moderately sized (428 nt) RNase H-sensitive R-loops. Our inability to detect such regions in native mtDNA R-loops indicates that they were either absent or structurally exclusive of our AFM and RNase H probing meth-

ods. However, light treatment of the complex with RNase A resulted in the formation of plectonemes and toroids, which are highly twisted DNA structures (Fig. 5*B*). This not only confirms the presence of RNA but also reveals that the mtRNA resulted in a redistribution of local supercoiling characteristics. To quantify this effect we counted the number of crossovers, which is a measure of visible DNA writhe in circular molecules. Strand crossovers can be counted from the AFM images where the Z-dimension topology is particularly sensitive. The distributed data are shown in Fig. 5, *C* and *D*. The median number of crossovers in the untreated sample is 14 (Fig. 5*C*) and in the sample treated with RNase is 33 (Fig. 5*D*); the two populations are significantly different by the ANOVA single factor analysis at a $p = 3.1 \times 10^{-5}$. It appears that the RNA formed an extensive triplex with limited hybridization to the mtDNA while maintaining the mtDNA in a more open conformation. The RNase treatment was not expected to affect the linking number. However, the mtRNA may have affected the distribution of supercoiling depending on how, when, and where the R-loops were formed.

DISCUSSION

We have purified and characterized mammalian mtDNA containing native R-loops. Although some of these RNA-DNA hybrids are involved in priming DNA replication, others are not. Rather, it appears that close association of mtRNA with mtDNA is a general feature of this genome. The extensive R-loops alter the local features of mtDNA conformation. This organization and the subsequent opportunities for various hetero- and homoduplex strand interactions under different circumstances are expected to have multiple consequences for the maintenance and expression of mtDNA.

The R-loops formed at the mitochondrial leading strand origin of replication, O_H, have been reconstituted previously and characterized *in vitro* (30). Here we show that native forms of this primer co-purify with the closed circular mtDNA template. There are two types of R-loops at O_H. A short ~150-nt RNA, which is neither extensively hybridized to the mtDNA nor extended by the mtDNA polymerase, may represent either a mature unused primer or a processed vestige for which the primer function has been completed. In either case, the major transition site between RNA and DNA lies just 3′ to this small CSB-limited RNA, which confirms prior data (27, 28). The second type of R-loop at O_H has several members, which comprise a larger ~575-nt population. These were extended by the mtDNA polymerase and are thus covalently linked RNA primer-DNA replicative initiation intermediates. They extend beyond CSBI and remain hybridized to the DNA template. DNase treatment revealed three predominant RNA to DNA transition sites within this population. The previously mapped O_H start site at CSBI (GenBank™ accession number NC_005089, nucleotide position ~16,034) is clearly the most abundant. The two other transition sites are defined by the DNase-insensitive RNA bands of ~525 and ~350 nt, which appear in Fig. 2, *A* and *B*. Assuming these transcripts begin at the light-strand transcription initiation site at nucleotide 16,188, their respective RNA to DNA transition sites would map in the area of mouse mtDNA nucleotides 15,650–15,850. Our sizing estimate places the 3′-end of the ~525-nt RNA transition near mouse mtDNA position 15,665. Interestingly, this site lies within a sequence element that would yield a very G-rich RNA, which implicates it as both an R-loop stability element and a potential RNA processing site. Alternatively, it is possible that this promoter distal transition site is one of the replication initiation sites identified by Yasukawa *et al.* (9) using ligation-mediated PCR, which would place the 3′-end at nucleotide position 15,625. The other more promoter-proximal transition site, identified here by the ~350-nt RNA, appears to be novel. Successful purification of the native O_H R-loops and the DNA extended form of those R-loops also serves to validate the strategy used here to search for relevant RNA-DNA hybrids at other locations within the mtDNA genome.

Other R-loops were found at a variety of positions on the mtDNA. We show here that RNAs from the COII, Cyt *b*, ND1, 16S rRNA, and ND6 genes all co-purify with mtDNA. There are several lines of evidence to indicate that these RNAs do not simply become attached to the DNA after lysis of the mitochondria. As shown in Fig. 1, the 16S rRNA, ND1, and ND6 RNAs are either located outside the displaced single-stranded region or are transcribed on the opposite strand of DNA (ND6). RNA association with mtDNA is therefore not limited to single DNA strands exposed during asymmetric replication. Rather, it appears to occur within the context of double-stranded mtDNA throughout the circular genome. Sequence analysis of the R-loops revealed that they are distinct in several ways from the total population of RNAs synthesized. For example, COII and Cyt *b* R-loops are more frequently truncated at the 3′-ends. Cyt *b* R-loops are also significantly more likely to be shorter at the 5′-ends. This indicates that the R-loops are either formed in a different manner or are subject to distinctive subsequent processing steps.

The R-loops are apparently not formed strictly by Watson-Crick base pairing and strand displacement. RNase H sensitivity indicates that the R-loops are less than fully hybridized. However, AFM imaging was unable to reveal free RNA ends or loosely attached RNA on the mtDNA. Nor were we able to detect by AFM extensive regions of RNA-DNA hybrid (supplemental Fig. S2). The AFM did reveal that the majority of the mtDNA molecules had enough RNA to significantly alter their apparent conformation. Thus, it appears that the RNA is largely intertwined within the DNA duplex, with oftentimes limited base pairing.

The mechanism for mitochondrial R-loop formation is unclear. This type of R-loop may result from transcription-induced DNA supercoiling similar to that found in *E. coli* (31). R-loop formation is also enhanced in other biological systems when normal RNA packaging and transport are disrupted. In *E. coli*, uncoupling of transcription and translation increases R-loop formation (32). In yeast, the THO-TREX complex plays several roles involving transcription elongation and RNA processing. Mutations within this complex lead to formation of R-loops and transcription associated hyper-recombination (14). Essentially the same phenotype occurs when the mammalian RNA splicing factor ASF/SF2 is inactivated (33). Finally, R-loops are also promoted by the human RNA capping enzyme,

extending the link between transcription, processing, and R-loops (34).

Previous studies have also indicated that RNA may be tightly associated with mtDNA. Attardi and colleagues (35, 36) purified mitochondrial transcription complexes associated with mtDNA more than 30 years ago. However, we sought here to identify more stably associated RNA that might be utilized as replication primers and not simply transcription complexes. Nevertheless, those studies (35, 36) estimated that 70% of mtDNA is actively being transcribed at a given moment, indicating that there is abundant RNA, which is at least associated with mtDNA. More recently, Iborra *et al.* (37) found that labeled mtRNA resides with mtDNA *in vivo* for an extended time. The *in vivo* association of RNA with mtDNA was also demonstrated using PUMILIO1 proteins engineered to bind to specific mitochondrial transcripts and highlight transcript location using split enhanced green fluorescent protein (38), an approach that revealed specifically that the mtDNA-encoded ND6 transcript remains associated with the mtDNA. However, in those studies limited spatial resolution made it unclear whether the RNA was trapped within the nucleoid complex or was in fact bound to the mtDNA. In the current study we have demonstrated that it is likely that at least some of the mtRNA is and remains stably bound to the mtDNA template.

Holt and colleagues (9, 24) have also found that RNA associates with partially purified mtDNA. However, those authors have concluded that these RNA molecules are replication intermediates, in which the light strand is synthesized via a long RNA intermediate, which is then converted by an unknown mechanism to DNA. This is termed the RITOLS replication model (an acronym for ribonucleotide incorporation throughout the lagging strand). The essential feature of this model is that most of the purported replicating forms of mtDNA identified by two-dimensional agarose gel patterns are fully double-stranded, with one of the nascent strands being RNA. We suggest that the RNA identified by Holt and co-workers (9, 24) does not represent a major replicative intermediate for several reasons. First, this model is inconsistent with previous data showing that RNA is not a major constituent of newly synthesized mtDNA. Newly replicated mtDNA was radiolabeled, isolated, and found not to have a disproportionate ribonucleotide incorporation (39), in contrast to what is predicted from the RITOLS model. The work presented here casts further doubt on the RITOLS model. DNase sensitivity indicates that neither the COII nor the Cyt *b* transcripts are detected as DNA-extended RNA primers. Rather, it appears that these and other transcripts are generally associated with duplex DNA throughout the genome on both strands. Furthermore, these RNAs are likely to have confounded interpretation of two-dimensional agarose gels by mimicking patterns commonly associated with replication intermediates. Holt and co-workers (9, 24) have described in particular those RNA-DNA hybrids that form with the single H-strand of DNA, which is displaced by the leading nascent replication strand synthesized between O_H and O_L. These form various patterns that mimic replication intermediates, including standard Y-arcs, slow moving Y-arcs, and bubbles, all of which are wholly or partially sensitive to RNase H treatment (9, 24). In agreement, the CsCl-gradient purified mtDNA used in this study also contains R-loops that are partially sensitive to RNase H. It is unclear whether this indicates partial hybridization or an RNase H-resistant R-loop conformation. In either case, if RNase digestion is incomplete, then what remains behind on a two-dimensional agarose gel cannot be unambiguously interpreted as fully duplex replicating DNA.

Although the bulk of the steady-state R-loops are not involved in replication, there is a significant population of RNAs that have an unmodified, free 3′-OH. It remains possible that these R-loop RNAs could be used as $^{alt}O_L$ replication primers, albeit at a low frequency. Although the current analysis failed to disclose discrete $^{alt}O_L$ replication primers, the finding that mitochondrial R-loops are heterogeneous and pervasive is critical in the $^{alt}O_L$ origin replication mechanism. Our hypothesis remains that the R-loop RNAs are used as fortuitous primers along the displaced single H-strand after initiation from O_H. The components of the $^{alt}O_L$ replisome and the mechanism of initiation remain to be determined. A step in this direction has recently been made by the finding that human mtRNA polymerase can synthesize short primer RNAs on single-stranded DNA *in vitro* (40). This may represent functional redundancy in the capacity to regulate alternative light-strand priming events using either longer, processed R-loops, or shorter primers. In addition, the longer R-loops may serve to limit the single-stranded DNA available for the mtRNA polymerase-mediated synthesis of shorter primers *in vivo*.

Acknowledgments—We greatly appreciate the contribution of Melissa Ramirez in the cloning and sequencing of the mtRNA cDNAs. We also thank Tom Jones for helpful discussions.

REFERENCES

1. Itoh, T., and Tomizawa, J. (1980) *Proc. Natl. Acad. Sci. U. S. A.* **77,** 2450–2454
2. Lee, D. Y., and Clayton, D. A. (1997) *Genes Dev.* **11,** 582–592
3. Lee, D. Y., and Clayton, D. A. (1998) *J. Biol. Chem.* **273,** 30614–30621
4. Xu, B. J., and Clayton, D. A. (1995) *Mol. Cell. Biol.* **15,** 580–589
5. Xu, B. J., and Clayton, D. A. (1996) *EMBO J.* **15,** 3135–3143
6. Clayton, D. A. (2003) *IUBMB Life* **55,** 213–217
7. Falkenberg, M., Larsson, N. G., and Gustafsson, C. M. (2007) *Annu. Rev. Biochem.* **76,** 679–699
8. Bowmaker, M., Yang, M. Y., Yasukawa, T., Reyes, A., Jacobs, H. T., Huberman, J. A., and Holt, I. J. (2003) *J. Biol. Chem.* **278,** 50961–50969
9. Yasukawa, T., Reyes, A., Cluett, T. J., Yang, M. Y., Bowmaker, M., Jacobs, H. T., and Holt, I. J. (2006) *EMBO J.* **25,** 5358–5371
10. Brown, T. A., Cecconi, C., Tkachuk, A. N., Bustamante, C., and Clayton, D. A. (2005) *Genes Dev.* **19,** 2466–2476
11. Brown, T. A., and Clayton, D. A. (2006) *Cell Cycle* **5,** 917–921
12. Pikó, L., Bulpitt, K. J., and Meyer, R. (1984) *Mech. Ageing Dev.* **26,** 113–131
13. Yu, K. F., Chedin, F., Hsieh, C. L., Wilson, T. E., and Lieber, M. R. (2003) *Nat. Immunol.* **4,** 442–451
14. Huertas, P., and Aguilera, A. (2003) *Mol. Cell* **12,** 711–721
15. Dasgupta, S., Masukata, H., and Tomizawa, J. (1987) *Cell* **51,** 1113–1122
16. Drolet, M. (2006) *Mol. Microbiol.* **59,** 723–730
17. Camps, M., and Loeb, L. A. (2005) *Front. Biosci.* **10,** 689–698
18. Tapper, D. P., Van Etten, R. A., and Clayton, D. A. (1983) *Methods Enzymol.* **97,** 426–434
19. Brown, T. A., and Clayton, D. A. (2002) *Nucleic Acids Res.* **30,** 2004–2010
20. Tautz, D., and Renz, M. (1983) *Anal. Biochem.* **132,** 14–19
21. Kusov, Y. Y., Shatirishvili, G., Dzagurov, G., and Gauss-Muller, V. (2001) *Nucleic Acids Res.* **29,** E57–57
22. Tomecki, R., Dmochowska, A., Gewartowski, K., Dziembowski, A., and

Stepien, P. P. (2004) *Nucleic Acids Res.* **32,** 6001–6014
23. Rivetti, C., Guthold, M., and Bustamante, C. (1999) *EMBO J.* **18,** 4464–4475
24. Yang, M. Y., Bowmaker, M., Reyes, A., Vergani, L., Angeli, P., Gringeri, E., Jacobs, H. T., and Holt, I. J. (2002) *Cell* **111,** 495–505
25. Kasamatsu, H., Robberson, D. L., and Vinograd, J. (1971) *Proc. Natl. Acad. Sci. U. S. A.* **68,** 2252–2257
26. Robberson, D. L., and Clayton, D. A. (1972) *Proc. Natl. Acad. Sci. U. S. A.* **69,** 3810–3814
27. Chang, D. D., Hauswirth, W. W., and Clayton, D. A. (1985) *EMBO J.* **4,** 1559–1567
28. Kang, D., Miyako, K., Kai, Y., Irie, T., and Takeshige, K. (1997) *J. Biol. Chem.* **272** 15275–15279
29. Slomovic, S., Laufer, D., Geiger, D., and Schuster, G. (2005) *Mol. Cell. Biol.* **25,** 6427–6435
30. Lee, D. Y., and Clayton, D. A. (1996) *J. Biol. Chem.* **271,** 24262–24269
31. Li, X. L., and Manley, J. L. (2006) *Genes Dev.* **20,** 1838–1847
32. Broccoli, S., Rallu, F., Sanscartier, P., Cerritelli, S. M., Crouch, R. J., and Drolet, M. (2004) *Mol. Microbiol.* **52,** 1769–1779
33. Li, X. L., and Manley, J. L. (2005) *Cell* **122,** 365–378
34. Kaneko, S., Chu, C., Shatkin, A. J., and Manley, J. L. (2007) *Proc. Natl. Acad. Sci. U. S. A.* **104,** 17620–17625
35. Aloni, Y., and Attardi, G. (1972) *J. Mol. Biol.* **70,** 363–373
36. Carré, D., and Attardi, G. (1978) *Biochemistry* **17,** 3263–3273
37. Iborra, F. J., Kimura, H., and Cook, P. R. (2004) *BMC Biol. 2004,* 2:9
38. Ozawa, T., Natori, Y., Sato, M., and Umezawa, Y. (2007) *Nat. Methods* **4,** 413–419
39. Bogenhagen, D., and Clayton, D. A. (1978) *J. Mol. Biol.* **119,** 69–81
40. Wanrooij, S., Fusté, J. M., Farge, G., Shi, Y., Gustafsson, C. M., and Falkenberg, M. (2008) *Proc. Natl. Acad. Sci. U. S. A.* **105,** 11122–11127